Supplementary material (ESI) for Journal of Materials Chemistry

Synthesis of Transition Metal Oxide Nanoparticles with Ultrahigh Oxygen Adsorption Capacity and Efficient Catalytic Oxidation Performance

Hui Zhang, Jian-Liang Cao, Gao-Song Shao, *and* Zhong-Yong Yuan*

Institute of New Catalytic Materials Science, College of Chemistry, Nankai University, Tianjin 300071, China. E-mail: zyyuan@nankai.edu.cn

Supporting Information

Characterizations of samples

Powder X-ray diffractions (XRD) were measured using a Rigaku D/max-2500 diffractometer with monochromatic Cu K_α radiation (λ=1.5418 Å). X-ray photoelectron spectroscopy (XPS) measurements were carried out on a PHI5300 spectrophotometer with Mg K_α radiation. The binding energy values were calibrated by using the C 1s level (284.6 eV) of the trace surface contaminants. Transmission electron microscopy (TEM) analysis was performed on a Philips Tecnai G20 microscope, operating at 200 kV. The surface areas were measured on a Quantachrome NOVA 2000e sorption analyzer by the BET method. The content of Na atoms was analyzed by inductively coupled plasma (ICP) emission spectroscopy on a Thermo Jarrell-Ash ICP-9000 (N + M) spectrometer.

Temperature-programmed reduction/desorption (TPR/TPD) experiments were preformed using a Quantachrome ChemBET-3000 analyzer with a thermal conductivity detector (TCD). H_2-TPR experiments were carried on under the mixture of 5% H_2 in N_2 flowing (30 mL/min) over 20 mg of catalyst at a heating rate of 10 ^oC/min. O_2-TPD measurements were performed up to 600°C with a

ramp of 10 ^{o}C/min in a 50 mL/min of helium flow. **Before the TCD detector, the out gas was passed through a pipe containing NaOH powder and cooled by an ice-salt bath to remove possible water vapor and carbon dioxide.** To convert the peak area data to volume data, the analyzer (TCD signal) was calibrated with pure oxygen of known volume.

Catalytic tests were performed in a continuous-flow fixed-bed microreactor at atmospheric pressure. The reaction gas mixture consisting of 10 vol.% CO balanced with air was passed through the catalyst bed at a total flow rate of 2.2 L/h. After 30 min reaction (stabilization time), the effluent gases were analyzed online by a GC-900A gas chromatograph equipped with a TCD detector. The activity was expressed by the conversion of CO (%).

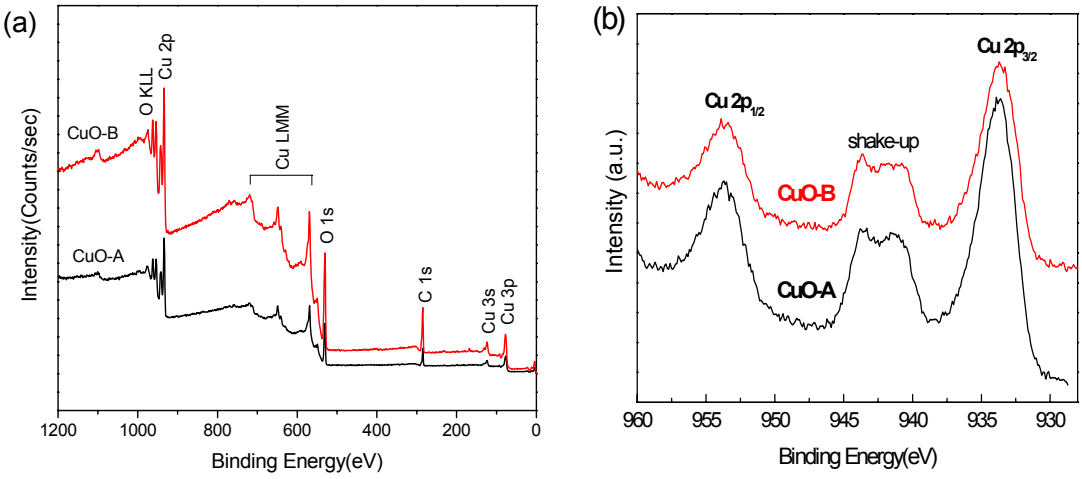

Figure S1. (a) The XPS spectra survey and (b) Cu 2p XPS spectra of **CuO-A** and **CuO-B** samples. The possible impurities of sodium and chlorine are not found. X-ray photoelectron spectra present the diagnostic shake-up peaks of CuO and the peaks of Cu 2p3/2 and Cu 2p1/2, indicating pure copper(II) oxide. The C 1s peak of the trace C-(C,H) components is widely used as calibration.

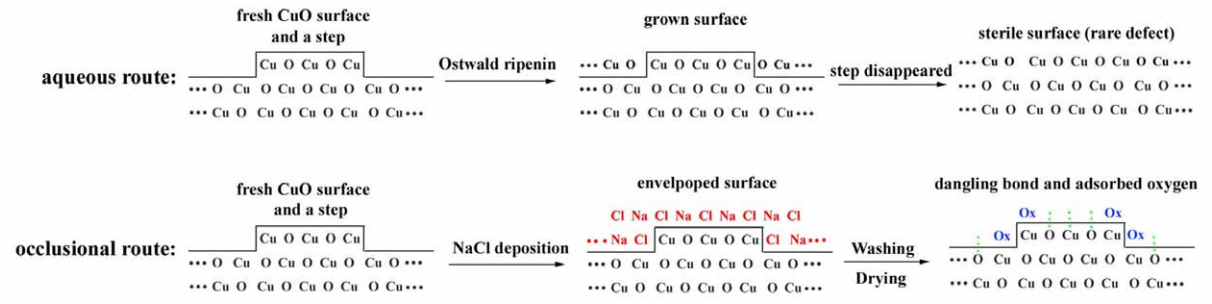

Figure S2. The protecting mechanism scheme of the occlusional coprecipitation strategy. The reaction of $CuCl_2$ and NaOH in nonaqueous condition resulted in numerous tiny fresh CuO nanoparticles, which have abundant surface defects (isolated atoms, voids, steps, etc). One step in the new-formed CuO surface is selected to illustrate the difference between the traditional synthesis route and the occlusional coprecipitation process. In aqueous solutions the crystallite growth and Ostwald ripening would result in an impoldered step and a repaired (disappeared) defect. In contrast, supersaturated sodium chloride in ethanol system would crystallize on the crystallization centres of the new-formed CuO nanoparticles, or to say, the synchronously-yielded NaCl adsorbs and deposits on the fresh surface of CuO nanoparticles, resulting in the coverage of NaCl, which can protect defects by blocking the mass transference. In a sense, the shield of NaCl is very much alike to the protective groups in organic synthesis. Thus abundant surface defects survive in the following treatments and can be rediscovered by removing NaCl shield. Due to the abundant defects and dangling bonds on the fresh surface, the synthesized CuO nanoparticles adsorb much oxygen molecules in air (in various species), showing ultrahigh adsorption capacity.

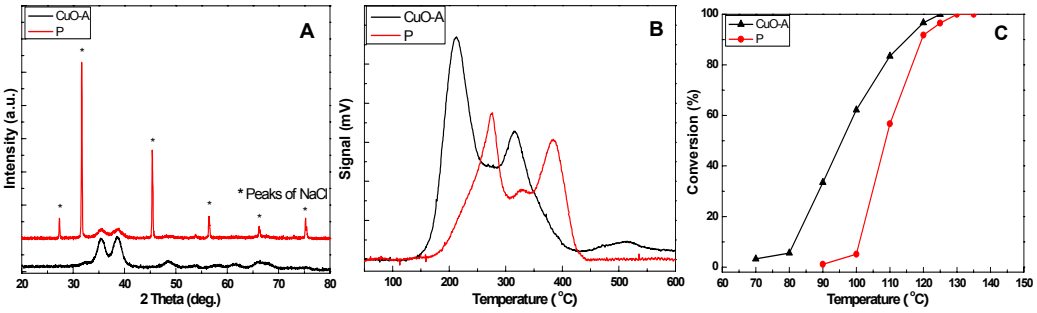

Figure S3. Comparison in the XRD patterns (A), the H_2-TPR curves (B) and the CO oxidation activity (C) of the as-product (**P**) and the corresponding sample **CuO-A**. The two reduction steps of the as-product (P, the enveloped CuO) presented at higher temperatures in contrast with the following washed sample (CuO-A), confirming the shield of NaCl has the ability to retard the reactions between CuO and hydrogen by blocking the mass transference of reagents. The obstructing effect of the NaCl shield also resulted in the lower conversion of CO for the as-product than the naked CuO nanoparticles.

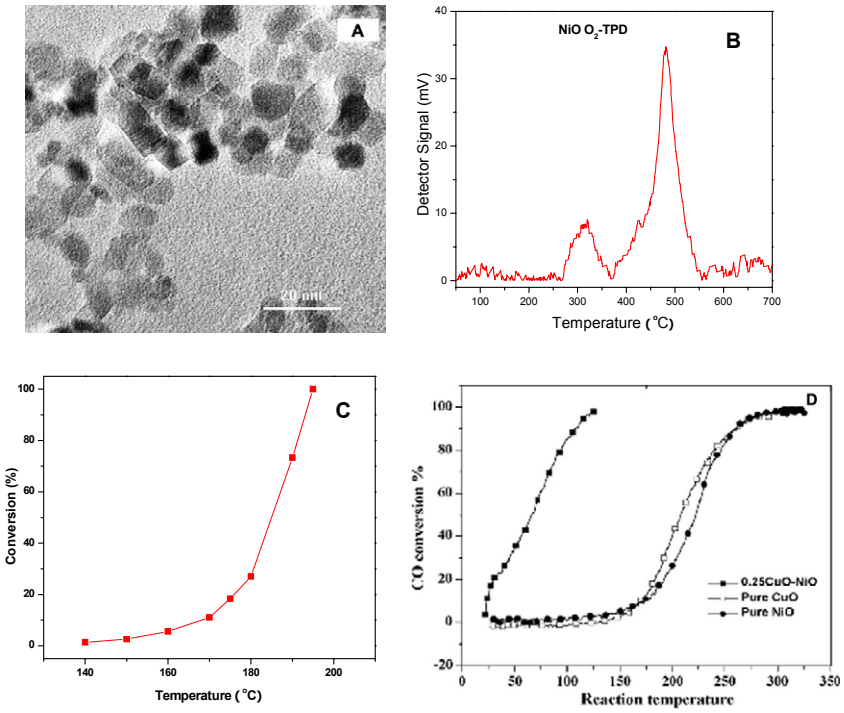

Figure S4. (A) Typical TEM image of the synthesized NiO sample. (B) The O_2-TPD curve of the synthesized NiO sample, showing two desorption peaks that should be assigned to the weakly and strongly chemisorbed oxygen. (C) The curve of the sample in CO catalytic test, having the total conversion temperature of about 195 ^{o}C. (D) The conversion curves of some catalysts cited from the literature [SR1]. It can be seen that the $T_{100\%}$ of pure NiO is about 290 ^{o}C.

Table S1. Some literature records of CuO based catalysts for carbon monoxide oxidation

Sample	Characterizations	$T_{100\%}$ (^oC)	Reference
CuO	Prepared by $Cu(NO_3)_3$ calcined at 500^oC	370	[SR1]
CuO		300	[SR2]
CuO	Nanoparticles	200	[SR3]
CuO	Nanobelt	150	[SR3]
CuO	Nanoplatelets	150	[SR3]
CuO		103	[SR4]
CuO/Al_2O_3		350	[SR5]
CuO/TiO_2		110	[SR6]
CuO/Fe_2O_3	Mesoporous CuO–Fe_2O_3 composite	110	[SR7]
$CuO/Ce_{0.8}Zr_{0.2}O_2$	Mesoporous $CuO/Ce_{0.8}Zr_{0.2}O_2$ catalysts	90	[SR8]
CuO-B		95	This work

Table S2. Some activation energy comparison of CuO based catalysts

Catalyst	Ea (KJ/mol)	Reference
CuO	54.5	[SR2]
CuO	92	[SR9]
$CuCr_2O_4$	97	[SR9]
$BaCuO_2$	63	[SR10]
$CuO.CuCr_2O_4$	84	[SR11]
CuO/cordierite	52.2	[SR12]
CuO-A	124	[SR13]
CuO-B	88.6	
$CuO-CeO_2$	40–50	[SR14]
$Cu_{0.1}Ce_{0.9}O_2$	59	[SR15]
$CuO{\cdot}MnO_x$	64.08 for 273–313K 12.15 for 333–373 K	[SR16]
CuO-A	52.7 for 70-80^oC 18.4 for 110-120^oC	This work
CuO-B	59.5 for 70-80^oC	This work

12.5 for 90-95^{o}C

References:

[SR1] X. Jiang, R. Zhou, J. Yuan, G. Lu, X. Zheng, *J. Chin. Rare Earth Soc.*, **2002**, *20(2)*, 111.

[SR2] A.K. Sharma, *J. Envir. Engrg*, **2006**, *132(8)*, 956.

[SR3] K. Zhou, R.Wang, B. Xu, Y. Li, *Nanotechnology*, **2006**, *17*, 3939.

[SR4] N.T. Thomas, L.S. Caretto, K. Nobe, *Ind. Eng. Chem. Process Des. Dev.*, **1969**, *8(2)*, 282.

[SR5] G. Pantaleo, L.F. Liotta, A.M. Venezia, G. Deganello, E.M. Ezzo, M.A. El Kherbawi, H. Atia, *Mater. Chem. Phys.*, **2008**, Inpress (doi:10.1016/j.matchemphys.2008.10.006).

[SR6] J. Huang, S. Wang, Y. Zhao, X. Wang, S. Wang, S. Wu, S. Zhang, W. Huang, *Catal. Commun.*, **2006**, *7*, 1029.

[SR7] J.L. Cao, Y. Wang, X.L. Yu, S.R. Wang, S.H. Wu, Z.Y. Yuan, *Appl. Catal. B*, **2008**, *79*, 26.

[SR8] J.L. Cao, Y. Wang, T.Y. Zhang, S.H. Wu, Z.Y. Yuan, *Appl. Catal.* B, **2008**, *78*, 120.

[SR9] Y. Yao, Y.-Fang., *J. Catal.*, **1975**, *39*, 104.

[SR10] I. Halasz, A. Brenner, M. Shelef, K.Y. Simon, *J. Catal.*, **1990**, *126*, 109

[SR11] W. Hertl, R. J. Farrauto, *J. Catal.*, **1973**, *29(2)*, 352

[SR12] H.G. El-Shobaky, Y.M. Fahmy, *Appl. Catal. B*, **2006**, *63*, 168

[SR13] U.R. Pillai, S. Deevi, *Appl. Catal.* B, **2006**, *64*, 146.

[SR14] G. Marban, A.B. Fuertes, *Appl. Catal.* B, **2005**, *57*, 43.

[SR15] G. Sedmak, S. Hcevar, J. Levec, *J. Catal.*, **2003**, *213*, 135.

[SR16] M. Li, D.-H. Wang, X.-C. Shi, Z.-T. Zhang, T.-X. Dong, *Sep. Purif. Technol.*, **2007**, *57*, 147.